Electron-impact excitation of ions in the magnesium sequence: Fe XV

R. B. Christensen,* D. W. Norcross,† and A. K. Pradhan
Joint Institute for Laboratory Astrophysics, University of Colorado and National Bureau of Standards, Boulder, Colorado 80309
(Received 12 March 1985)

Intermediate-coupling collision strengths are calculated for all transitions between the states $3s^2\,{}^1S_0$, $3s3p\,({}^3P_{0,1,2}, {}^1P_1)$, $3p^2({}^1D_2, {}^3P_{0,1,2}, {}^1S_0)$, $3s3d\,({}^3D_{1,2,3}, {}^1D_2)$, and $3s4s\,({}^3S_1, {}^1S_0)$. Calculations are carried out in a ten-state distorted-wave approximation. Resonance effects are considered by using multichannel quantum-defect theory, and relativistic effects in the target Hamiltonian are taken into account in the Breit-Pauli formulation. The important $3s^2\,{}^1S_0-3s3p\,{}^3P_1$ transition is found to be subject to large resonance enhancement, as previously shown by other workers for less highly charged Mg-like ions. Term coupling among the target states also affects several transitions considerably. Present results are compared with previous calculations; some significant differences are noted. The new results suggest a serious discrepancy between calculated and observed relative intensities of the 284.2-Å (resonance) and 417.3-Å (intercombination) lines for Fe XV in the Sun, but will reduce the discrepancy for this ratio for other Mg-like ions observed in tokamak plasmas.

I. INTRODUCTION

Ions of the magnesium isoelectronic sequence are important sources of uv line radiation in a number of astrophysical sources, e.g., the Sun.[1,2] In addition, certain transitions in these ions are also observed in laboratory sources.[3] For example, wavelengths of the semiforbidden (or intercombination) line $3s3p\,{}^3P_1-3s^2\,{}^1S_0$, at 417.3 Å in Fe XV, have recently been determined from measurements[3,4] in tokamak discharges for ten Mg-like ions. These and other measurements, however, consistently point out discrepancies between calculated and measured ratios of the intensity of this line and that of the allowed resonance line, at 284.2 Å in Fe XV. Being relatively insensitive to either electron temperature or density, this ratio is not in itself a very useful diagnostic tool, but rather a good test of the atomic data. These discrepancies should, therefore, be resolved if models based on collision data such as presented in this paper are to be reliably used as diagnostic tools for either astrophysical or laboratory plasmas.

Accurate calculations have been previously carried out for the lower members of the sequence, $_{14}$Si III and $_{16}$S V (Refs. 5 and 6, respectively), in the close-coupling approximation, including the extensive resonance structure that affects particularly the ${}^1S_0$-${}^3P_1$ transition. These calculations were done in the *LS* coupling approximation, and included extensive configuration-interaction (CI) effects. However, in the present work we deal with a highly charged Mg-like ion where it is also necessary to employ an intermediate-coupling (IC) scheme and to allow for relativistic effects. In addition, since resonances have been shown to play an important role in the inelastic scattering for several transitions, it is also necessary to consider the resonant process in order to obtain accurate cross sections.

There have been a series of increasingly more sophisticated calculations of cross sections for electron-impact excitation of Fe XV over the years.[7–13] The first[7] of these employed the Coulomb-Born approximation, neglected CI, but included some relativistic effects. The importance of resonances in Fe XV was first appreciated by the authors of that paper, and they made an attempt to estimate their effect. This is an issue returned to only in the present work. Later work pointed out the potential importance of cross sections for transitions neglected earlier, specifically the spin-forbidden transitions $3s^2\,{}^1S_0-3s3d\,{}^3D_J$ (Ref. 9) and $3s^2\,{}^1S_0-3p^2\,{}^3P_2$ (Ref. 12).

The most recent calculations[12,13] included extensive CI in the target, and employed the distorted-wave (DW) method to solve the scattering problem in *LS* coupling. Fine-structure collision strengths were obtained by a subsequent transformation to an IC scheme, with the inclusion of relativistic term coupling coefficients from the target. The calculations of Bhatia and Kastner[12] were carried out with essentially the same program package (developed at University College, London[14]) as employed in the present work. Our calculations are not fundamentally different than these two recent studies, but we adopt a much more extensive CI basis for the target, and include the effect of resonances using quantum-defect theory (QDT).

As the channel coupling becomes weaker with nuclear charge Z (the reactance matrix elements $R_{ii'}$ are $\propto Z^{-1}$), the DW approximation is often comparable in accuracy to the more time-consuming close-coupling method for the higher members of a given isoelectronic sequence (see, for example, our earlier calculations for the helium isoelectronic sequence[15–18]). However, as shown in the references on the helium sequence work, certain important atomic effects such as autoionization (AI), IC and, in some instances, dielectronic recombination (DR), need to be taken into consideration. For the magnesium sequence it is already known that AI and IC effects are important, but we do not expect the DR effect on excitation cross sections to be appreciable, since the radiative transition probabilities for the allowed transitions between the lowest ten states are less than $\sim 2\times 10^{11}$ s^{-1} (the A value for the $3s3p\,{}^1P_1\rightarrow 3s^2\,{}^1S_0$ resonance transition), and

would not effectively compete with AI probabilities that are usually in the range 10^{12}–10^{14} s^{-1} for the low-lying autoionizing states.

In the present work we calculate collision strengths for a larger number of transitions than in earlier calculations and incorporate additional atomic effects, mentioned above, that should yield more accurate results. We conclude, in particular, that resonances increase the effective cross section for the $3s^2\,{}^1S_0$–$3s\,3p\,{}^3P_1$ transition in the important resonance region by more than a factor of 2 over previous nonresonant results.[7,9,12,13] Cross sections for other transitions that effectively populate the $^3P_1$ states by radiative cascade are also found to be larger. Both effects will tend to substantially increase the calculated emission from the $^3P_1$ state.

II. METHOD AND CALCULATIONS

The DW method, as incorporated in the University College, London, program package, has been described in Ref. 14 and in our calculations on He-like ions.[15–18] Here we, therefore, confine ourselves to giving the computational details of the atomic structure and the scattering calculations.

A. Atomic structure

We employ the SUPERSTRUCTURE code of Eissner *et al.*[19] The target basis set of eigenstates consists of ten *LS* states which are (giving the dominant configuration) $3s^2(^1S)$, $3s\,3p(^3P,{}^1P)$, $3p^2(^3P,{}^1D,{}^1S)$, $3s\,3d(^3D,{}^1D)$, and $3s\,4s(^3S,{}^1S)$. In addition to the "principal" configurations given above, a number of "correlation" configurations are also included in the target representation (cross sections involving terms dominated by the correlation configurations are not considered in the solution of the scattering problem). These are

$$\{3s\,5s, 3s\,4d, 3p\,4p, 3p\overline{4f}, 3d^2, 3d\,4d, 4p^2, 4d^2\}$$

for even parity ,

$$\{3s\,4p, 3p\,4s, 3p\,5s, 3p\,3d, 3p\,4d, 3d\,4p, 3d\overline{4f}\}$$

for odd parity .

The basis set of one-electron orbitals is calculated in a scaled Thomas-Fermi-Dirac-Amaldi potential, $V(\lambda_l,r)$, where λ_l are the scaling parameters for each l. The $\overline{4f}$ orbital is a nonspectroscopic orbital, scaled so as to approximate the correlation effect from the infinity of high-lying states; one such nonspectroscopic configuration is included for each parity. Variational minimization of the exact nonrelativistic Hamiltonian over a weighted sum of the lowest *LS* term energies in each symmetry yields initial values for the λ_l's. As we are interested in the fine-structure substates of the target, we then carry out a relativistic structure calculation, in the Breit-Pauli approximation. The initial λ_l's are slightly adjusted to improve agreement between calculated energies and dipole line strengths and some observed, or more accurate calculated, values. The scaling parameters finally adopted are the following: $\lambda_s=1.125$, $\lambda_p=1.044$, $\lambda_d=1.051$, and $\lambda_f=6.175$.

In Table I we give the calculated and observed energies for the target states. The former are given both before (*LS*) and after (*IC*) the relativistic terms are introduced into the Hamiltonian. The accuracy of the collision calculation is directly proportional to the accuracy of the target representation, i.e., the wave functions of the included target states. A reliable indication of the error in the wave functions may also be obtained by comparing the calculated electron dipole ($E1$) line strengths with observed values or other accurate calculations. Cheng and Johnson[21] have carried out relativistic multiconfiguration calculations for the line strengths of a number of dipole transitions in Mg-like ions. These are compared with our calculated line strengths, and those of Bhatia and Kastner[12] and Mann,[13] in Table II. For only one transition do our results differ from the results of Cheng and Johnson by more than 5%.

The largest difference is for the $3s^2\,{}^1S_0$–$3s\,3p\,{}^3P_1$ transition. Cheng and Johnson did not include any excitations out of the $n=3$ shell in their basis, but we find that the $3s\,4p$ configuration contributes substantially to our $3s\,3p\,{}^3P_1$ eigenfunction, accounting for most of the difference. The $3s\,4p$ configuration contributes much less significantly to any other of the transitions given in Table II; the agreement for these is generally excellent.

Transition probabilities for $E1$ transitions are given in Table III, along with previously recommended data.[22] There are no published data for three transitions, to our knowledge. Of the remaining 30 transitions, the agreement is better than 4% for 21; for only six transitions does the disagreement exceed 8%. The $3s^2\,{}^1S_0$–$3s\,3p\,{}^3P_1$ transition has already been discussed. Of the other five transitions, the recommended values for three (4-13, 4-15,

TABLE I. Target term energies for Fe XV (in Rydbergs) from measurements (Obs), and from the present calculation in *LS* and intermediate coupling (IC).

Index	State	$C_iS_iL_iJ_i$	$E^{\rm Obs}(S_iL_iJ_i)$[a]	$E^{\rm IC}(S_iL_iJ_i)$	$E^{LS}(S_iL_i)$
1	$3s^2\,{}^1S_0$		0.0	0.0	0.0
2	$3s\,3p\,{}^3P_0$		2.132	2.120	2.079
3	$^3P_1$		2.184	2.172	2.079
4	$^3P_2$		2.313	2.296	2.079
5	$^1P_1$		3.207	3.239	3.063
6	$3p^2\,{}^1D_2$		5.100	5.101	4.818
7	$^3P_0$		5.053	5.068	4.883
8	$^3P_1$		5.145	5.154	4.883
9	$^3P_2$		5.302[b]	5.303	4.883
10	$^1S_0$		6.012[b]	6.056	5.700
11	$3s\,3d\,{}^3D_1$		6.186	6.213	5.964
12	$^3D_2$		6.195	6.225	5.964
13	$^3D_3$		6.209	6.242	5.964
14	$^1D_2$		6.945	7.013	6.730
15	$3s\,4s\,{}^3S_1$		16.072	16.086	15.908
16	$^1S_0$			16.320	16.134

[a]Reference 20.

[b]Corrected as suggested in Ref. 12, see text.

TABLE II. Electric dipole line strengths for $_{26}$Fe XV (in a.u.). The figure in parentheses is the power of 10 by which the number is multiplied.

	$3s\,3p$:	$^3P_0$	$^3P_1$	$^3P_2$	$^1P_1$
$3s^2\,^1S$	a		4.4(−3)		7.53(−1)
	b		4.08(−3)		7.54(−1)
	c		3.0(−3)		7.43(−1)
	d		5.11(−3)		7.70(−1)
$3p^2\,^1D_2$	a		8.28(−2)	1.67(−1)	4.26(−1)
	b		8.35(−2)	1.73(−1)	4.35(−1)
	c		7.2(−2)	1.57(−1)	4.16(−1)
$3p^2\,^3P_0$	a		2.80(−1)		3.8(−3)
	b		2.82(−1)		3.68(−3)
	c		3.12(−1)		4.8(−3)
$3p^2\,^3P_1$	a	2.84(−1)	2.12(−1)	3.51(−1)	1.3(−3)
	b	2.84(−1)	2.12(−1)	3.53(−1)	1.29(−3)
	c	3.12(−1)	2.33(−1)	3.90(−1)	1.05(−3)
$3p^2\,^3P_2$	a		2.75(−1)	8.91(−1)	9.62(−2)
	b		2.76(−1)	8.88(−1)	9.80(−2)
	c		3.21(−1)	1.012	7.2(−2)
$3p^2\,^1S_0$	b		1.85(−3)		3.42(−1)
	c		1.1(−3)		4.97(−1)

[a]Reference 21.
[b]Present work.
[c]Reference 12.
[d]Reference 13.

and 5-16) were obtained with a Hartree-Fock-Slater program; our results are thus probably more accurate. The other two transitions for which significant differences exist (4-14 and 5-12) are spin-forbidden, have small transition probabilities, and are more sensitive to relativistic effects; we can express no preference in these cases.

This stage of the calculations also produced transition probabilities for all the electric quadrupole and magnetic dipole ($M1$) transitions among the 16 states considered. Of these only the $M1$ transition $3s\,3p\,^3P_2$—$3s\,3p\,^3P_1$ at 7058.6 Å is of practical interest, the others initiating in states that are not metastable and hence decay much fas-

TABLE III. Transition probabilities (in s^{-1}) for electric dipole transitions in $_{26}$Fe XV.

Transition				Transition			
i	j	A_{ji}[a]	A_{ji}[b]	i	j	A_{ji}[a]	A_{ji}[b]
1	3	3.79(7)	4.1(7)	4	9	1.27(10)	1.27(10)
1	5	2.22(10)	2.20(10)	4	11	6.02(8)	6.20(8)
2	8	6.95(9)	6.93(9)	4	12	5.49(9)	5.45(9)
2	11	1.38(10)	1.38(10)	4	13	2.21(10)	2.39(10)
2	15	3.45(10)	3.20(10)	4	14	1.27(7)	1.10(7)
3	6	1.11(9)	1.1(9)	4	15	1.81(11)	1.60(11)
3	7	1.79(10)	1.77(10)	5	6	1.58(9)	1.55(9)
3	8	4.90(9)	4.91(9)	5	7	6.19(7)	6.4(7)
3	9	4.48(9)	4.46(9)	5	8	8.39(6)	8.4(6)
3	10	2.77(8)		5	9	4.83(8)	4.7(8)
3	11	9.90(9)	9.90(9)	5	10	2.02(10)	2.02(10)
3	12	1.80(10)	1.80(10)	5	11	2.56(7)	2.40(7)
3	14	2.97(8)	3.00(8)	5	12	1.61(7)	1.40(7)
3	15	1.04(11)	9.80(10)	5	14	4.22(10)	4.19(10)
3	16	7.12(8)		5	15	8.07(8)	
4	6	2.00(9)	2.0(9)	5	16	2.13(11)	1.90(11)
4	8	7.16(9)	7.11(9)				

[a]Present work, using calculated line strengths and observed energy differences.
[b]Reference 22.

ter by $E1$ transitions. Our result for the transition probability is 38.1 s^{-1}, in good agreement with the recommended[23] value of 37.7 s^{-1}.

B. Scattering calculations

The scattering calculations are carried out for incident electron partial waves $l \leq 11$, which was assumed to yield adequate convergence in the LS collision strengths for all nondipole transitions. The scaling parameters in the continuum orbitals are taken to be the same as for the bound orbitals. The spin and angular symmetries with the above partial-wave expansion are as follows:

$$^{(2S+1)}(L)^{\pi} = {}^{4,2}(0,1,2,\ldots,11)^{e,o} ,$$

where the $^{(2S+1)}(L)^{\pi}$ denotes the total (electron + ion) spin state, the total angular momentum, and parity. The total L values are given in the bracket on the right-hand side, where e and o denote even- and odd-parity states. The calculations are first done for each symmetry in the nonresonant region above all thresholds at a few energies.

The LS reactance matrices thus obtained are transformed to the IC scheme employing the program JAJOM (Ref. 24) and including the term coupling coefficients from SUPERSTRUCTURE; thus incorporating relativistic effects from the target Hamiltonian. The transformation proceeds by an initial transformation of the reactance matrices from LS to pair coupling according to

$$\mathbf{R}^{J\pi}(S_iL_iJ_ilK;S_i'L_i'J_i'l'K') = \sum_{S,L} X(SLJ,S_iL_iJ_i,lK)R^{SL\pi}(S_iL_ils;S_i'L_i'l's') \times X(SLJ,S_i'L_i'J_i';l'K') , \quad (1)$$

where the X are products of Racah recoupling coefficients for the following pair coupling scheme:

$$S_i + L_i = J_i, \quad J_i + l = K, \quad K + s = J\pi . \quad (2)$$

The $\mathbf{R}^{J\pi}$ are then multiplied by the term coupling coefficients and the IC $\mathbf{R}^{J\pi}$ are obtained, i.e.,

$$\mathbf{R}^{J\pi}(\Delta_iJ_ilK,\Delta_i'J_i'l'K') = \sum_{\substack{S_i,L_i,\\ S_i',L_i'}} t_{J_i}(\Delta_i,\Gamma_iS_iL_i)\mathbf{R}^{J\pi}(S_iL_iJ_ilK;S_i'L_i'l'K') \times t_{J_i'}(\Delta_i,\Gamma_iS_i'L_i') , \quad (3)$$

where the t_{J_i} are the term coupling coefficients

$$t_{J_i}(\Delta_i,\Gamma_iS_iL_i) = \sum_{C_i,\beta_i} a^{S_iL_i}(\Gamma_i,C_i\beta_i)b^{J_i}(\Delta_i,C_i\beta_iS_iL_i) , \quad (4)$$

given in terms of the $a^{S_iL_i}$ representing the configuration mixing coefficients in LS coupling (nonrelativistic Hamiltonian) and the b^{J_i} that are the diagonalization coefficients for the Breit-Pauli Hamiltonian. The Γ_i and Δ_i label LS coupling and IC terms, C_i the configurations, and β_i the degeneracy parameters for multiple LS terms with the same C_i. The point to note is that an accurate CI representation is necessary in order to properly take account of relativistic term coupling among the target states (this point is discussed further in Sec. III; see also Ref. 19).

For allowed dipole transitions, convergence is not achieved by the partial wave summation in the DW calculations alone. The higher partial waves can be adequately considered in the Coulomb-Bethe approximation as described by Burgess and Sheorey.[25] The contribution for incident $l = 12, \infty$ is thereby calculated, using the calculated line strengths. There is some error introduced in this procedure for including high partial waves by the fact that the total symmetries in pair coupling (as employed in JAJOM) do not exactly match the last few symmetries in LS coupling and some higher partial waves (e.g., $l = 11$) are not fully taken into account. However, since the contribution from any given l value (particularly at large l) is small, this error is not very significant for the final collision strengths for the allowed transitions (we have determined it to be less than 5%).

The DW method does not allow for channel coupling directly; therefore resonances, which result from coupling between open and closed channels, are not present in the DW reactance matrices and hence cross sections. One may, however, employ quantum-defect theory (hereafter, QDT) in order to compute resonance structures and resonance averaged collision strengths, as has been described in a number of earlier works (e.g., Ref. 15). The program JAJOM was extended by Pradhan (JAJOM II, unpublished), employing QDT, to obtain detailed and averaged resonance structure in fine-structure collision strengths.

We use JAJOM II to calculate the detailed and averaged collision strengths including resonance contributions from the partial waves $l = 0$, 1, 2, 3, and 4 (the contribution from resonances with $l > 4$ is expected to be negligible). The procedure involves the extrapolation of the $\mathbf{R}^{LS}$ matrices, calculated above threshold, to energies below threshold and subsequent transformation to $\mathbf{R}^{J}$. QDT formulas given by Martins and Seaton[26] are then used to compute the detailed collision strengths with resonances belonging to the Rydberg series converging onto the threshold from below. The theory described by Gailitis[27] is used to compute resonance-averaged cross sections.

III. RESULTS AND DISCUSSION

In order to provide the collision strengths over a wide energy range, we have carried out the calculations at a number of energies above all thresholds. In Tables IV and V we give the collision strengths for the 120 transitions under consideration, including fine structure, at six energies (from the initial DW calculations, relative to the ground state) going up to at least six times the threshold energy. The highest electron energy used is about three times the ionization energy of Fe XV, and more than six times the energy corresponding to the coronal temperature (temperature of maximum abundance).

In Table IV we compare our results with those of Bhatia and Kastner[12,28] for all transitions listed by those au-

TABLE IV. Collision strengths for Fe XV: comparison of present (P) results with those of Refs. 12 and 28, denoted BK.

Transition $i \rightarrow j$		Ω^P (15.918 Ry)	Ω^{BK} (16.00 Ry)	Ω^P (25.19 Ry)	Ω^{BK} (24.00 Ry)
1	2	2.61(−3)	2.40(−3)	1.81(−3)	1.20(−3)
1	3	2.90(−2)	2.20(−2)	2.50(−2)	1.82(−2)
1	4	1.29(−2)	1.21(−2)	8.96(−3)	6.00(−3)
(1	5)[a]	2.77	2.77	3.04	2.70
1	6	8.18(−2)	7.73(−2)	7.98(−2)	5.11(−2)
1	7	7.78(−5)		6.86(−5)	
1	8	5.27(−5)		3.85(−5)	
1	9	1.77(−2)	1.33(−2)	1.74(−2)	8.90(−3)
1	10	1.92(−3)	2.40(−3)	1.76(−3)	1.70(−3)
1	11	7.49(−3)	6.10(−3)	4.73(−3)	3.80(−3)
1	12	1.25(−2)	1.02(−2)	7.92(−3)	6.20(−3)
1	13	1.75(−2)	1.43(−2)	1.10(−2)	8.40(−3)
1	14	1.92(−1)	1.55(−1)	1.84(−1)	1.03(−1)
1	15	3.40(−3)		2.10(−3)	
1	16			9.65(−2)	
2	3	3.06(−2)	1.82(−2)	1.40(−2)	8.40(−3)
2	4	1.06(−1)	7.96(−2)	9.50(−2)	4.77(−2)
2	5	4.21(−3)	2.90(−3)	2.24(−3)	1.40(−3)
2	6	1.13(−2)	8.30(−3)	6.17(−3)	4.00(−3)
2	7	1.77(−3)	1.70(−3)	1.26(−3)	9.00(−4)
(2	8)	1.20	1.29	1.33	1.23
2	9	1.46(−3)	8.00(−4)	5.99(−4)	4.00(−4)
2	10	3.97(−4)		2.21(−4)	
2	11	8.54(−1)	9.40(−1)	9.41(−1)	8.67(−1)
2	12	7.68(−3)	6.90(−3)	4.73(−3)	3.20(−3)
2	13	1.46(−2)	1.31(−2)	1.40(−2)	7.40(−3)
2	14	7.08(−3)	3.20(−3)	2.29(−3)	1.60(−3)
2	15	4.09(−3)[b]		6.71(−3)	
2	16			3.54(−4)	
3	4	3.10(−1)	2.00(−1)	2.28(−1)	1.25(−1)
3	5	1.86(−2)	1.12(−2)	9.51(−3)	5.60(−3)
3	6	3.29(−1)	3.21(−1)	3.93(−1)	3.05(−1)
(3	7)	1.16	1.32(0)	1.43(0)	1.27(0)
(3	8)	9.46(−1)	9.76(−1)	1.03(0)	9.33(−1)
(3	9)	1.03(0)	1.31(0)	1.22(0)	1.28(0)
3	10	8.33(−3)	4.90(−3)	9.00(−3)	4.30(−3)
(3	11)	6.12(−1)	7.16(−1)	7.31(−1)	6.59(−1)
(3	12)	1.69(0)	2.14(0)	2.04(0)	2.04(0)
3	13	4.04(−2)	3.61(−2)	3.48(−2)	1.92(−2)
3	14	3.68(−2)	2.45(−2)	2.49(−2)	1.87(−2)
(3	15)	1.23(−2)[b]		2.04(−2)	
3	16			1.15(−3)	
4	5	2.41(−2)	1.62(−2)	1.35(−2)	7.60(−3)
4	6	8.02(−1)	7.03(−1)	8.66(−1)	6.70(−1)
4	7	2.03(−3)	2.00(−3)	1.36(−3)	1.00(−3)
(4	8)	1.77(0)	1.66(0)	1.83(0)	1.61(0)
(4	9)	3.81(0)	4.21(0)	4.21(0)	4.05(0)
4	10	4.23(−3)	2.90(−3)	2.61(−3)	1.70(−3)
(4)	11)	7.26(−2)	7.48(−2)	7.92(−2)	6.19(−2)
(4	12)	7.01(−1)	7.63(−1)	7.66(−1)	7.09(−1)
(4	13)	3.28(0)	4.07(0)	3.64(0)	4.02(0)
4	14	3.62(−2)	1.62(−2)	1.23(−2)	7.50(−3)
(4	15)	2.08(−2)[b]		3.51(−2)	
4	16			1.77(−3)	
(5	6)	2.14(0)	2.22(0)	2.38(0)	2.24(0)
5	7	2.23(−2)	1.16(−2)	2.33(−2)	6.40(−3)
5	8	1.68(−2)	9.10(−3)	1.36(−2)	4.70(−3)
5	9	4.73(−1)	3.74(−1)	5.21(−1)	3.71(−1)

TABLE IV. (*Continued*).

Transition $i \rightarrow j$	Ω^P (15.918 Ry)	Ω^{BK} (16.00 Ry)	Ω^P (25.19 Ry)	Ω^{BK} (24.00 Ry)
(5 10)	1.55(0)	2.16(0)	1.71(0)	2.07(0)
5 11	2.09(−2)	1.30(−2)	1.34(−2)	6.50(−3)
5 12	3.13(−2)	2.01(−2)	1.85(−2)	9.70(−3)
5 13	3.68(−2)	2.47(−2)	1.83(−2)	1.11(−2)
(5 14)	5.32(0)	7.02(0)	5.93(0)	6.76(0)
5 15	6.36(−3)[b]		2.75(−3)	
(5 16)			1.66(−2)	
6 7	4.71(−2)	3.52(−2)	4.30(−2)	2.22(−2)
6 8	6.24(−2)	5.14(−2)	5.71(−2)	3.07(−2)
6 9	2.07(−1)	1.59(−1)	1.82(−1)	1.03(−1)
6 10	1.84(−1)	1.57(−1)	1.72(−1)	9.86(−2)
6 11	6.36(−3)	6.11(−3)	3.73(−3)	2.30(−3)
6 12	1.07(−2)	1.04(−2)	6.46(−3)	3.90(−3)
6 13	1.51(−2)	1.47(−2)	9.49(−3)	5.40(−3)
6 14	3.19(−2)	2.57(−2)	2.35(−2)	1.37(−2)
6 15	2.77(−3)		9.73(−4)	
6 16			4.16(−3)	
7 8	2.22(−2)	2.09(−2)	2.32(−2)	1.12(−2)
7 9	5.74(−2)	5.81(−2)	5.85(−2)	3.68(−2)
7 10	6.14(−4)	5.90(−4)	3.62(−4)	3.10(−4)
7 11	5.18(−4)	4.44(−4)	3.61(−4)	2.00(−4)
7 12	1.07(−3)	6.20(−4)	9.92(−4)	3.90(−4)
7 13	8.95(−5)	3.90(−5)	2.56(−5)	2.00(−5)
7 14	3.69(−3)	3.90(−3)	3.04(−3)	2.40(−3)
7 15	2.54(−5)		1.97(−5)	
7 16			1.51(−5)	
8 9	1.97(−1)	1.85(−1)	1.96(−1)	1.11(−1)
8 10	2.74(−3)	2.43(−3)	1.78(−3)	1.43(−3)
8 11	1.85(−3)	1.20(−3)	1.66(−3)	6.70(−4)
8 12	1.44(−3)	1.20(−3)	1.06(−3)	5.50(−4)
8 13	1.63(−3)	9.20(−4)	1.51(−3)	5.80(−4)
8 14	5.92(−3)	5.80(−3)	3.92(−3)	3.30(−3)
8 15	7.00(−5)		5.84(−5)	
8 16			5.02(−6)	
9 10	5.92(−2)	4.01(−2)	5.35(−2)	2.58(−2)
9 11	1.94(−3)	1.53(−3)	1.43(−3)	6.10(−4)
9 12	4.33(−3)	3.11(−3)	3.33(−3)	1.40(−3)
9 13	7.44(−3)	7.20(−3)	5.52(−3)	4.30(−3)
9 14	1.35(−2)	1.14(−2)	9.08(−3)	6.40(−3)
9 15	7.15(−4)		3.05(−4)	
9 16			9.32(−4)	
10 11	8.00(−4)	2.00(−4)	1.94(−4)	1.20(−4)
10 12	1.45(−3)	3.80(−4)	4.54(−4)	2.30(−4)
10 13	1.87(−3)	4.54(−4)	4.81(−4)	2.70(−4)
10 14	7.78(−2)	1.15(−2)	7.56(−2)	7.18(−2)
10 15	7.90(−5)		1.47(−5)	
10 16			1.58(−4)	
11 12	1.89(−1)	1.52(−1)	1.32(−1)	8.64(−2)
11 13	6.08(−2)	4.44(−2)	3.46(−2)	2.14(−2)
11 14	3.20(−2)	2.83(−2)	1.91(−2)	1.02(−2)
11 15	1.14(−2)		1.04(−2)	
11 16			9.30(−4)	
12 13	2.52(−1)	1.99(−1)	1.67(−1)	1.14(−1)
12 14	5.31(−2)	4.71(−2)	3.18(−2)	1.70(−2)
12 15	1.92(−2)		1.79(−2)	

TABLE IV. (*Continued*).

Transition $i \rightarrow j$	Ω^P (15.918 Ry)	Ω^{BK} (16.00 Ry)	Ω^P (25.19 Ry)	Ω^{BK} (24.00 Ry)
12 16			1.55(−3)	
13 14	7.41(−2)	6.56(−2)	4.44(−2)	2.36(−2)
13 15	2.71(−2)		2.59(−2)	
13 16			2.17(−3)	
14 15	7.25(−3)		3.49(−3)	
14 16			8.57(−3)	
15 16			3.45(−3)	

[a]Transitions in ( ) are spin- and dipole-allowed.
[b]*LS* energies, instead of the IC, are adopted in calculating the Coulomb-Bethe contribution from $l \geq 12$ for these transitions at 15.918 Ry.

TABLE V. Collision strengths for $_{26}$Fe XV.

Transition $i \rightarrow j$	26.95 Ry	50.38 Ry	64.14 Ry	96.21 Ry
1 2	1.20(−3)	8.22(−4)	5.99(−4)	3.36(−4)
1 3	2.86(−2)	2.91(−2)	2.96(−2)	3.13(−2)
1 4	5.93(−3)	4.06(−3)	2.96(−3)	1.65(−3)
1 5	3.76(0)	4.05(0)	4.31(0)	4.77(0)
1 6	7.80(−2)	7.53(−2)	7.22(−2)	6.52(−2)
1 7	5.65(−5)	4.58(−5)	3.79(−5)	2.56(−5)
1 8	2.42(−5)	1.50(−5)	1.01(−5)	4.82(−6)
1 9	1.70(−2)	1.64(−2)	1.58(−2)	1.43(−2)
1 10	1.53(−3)	1.30(−3)	1.10(−3)	7.64(−4)
1 11	3.13(−3)	2.12(−3)	1.51(−3)	8.06(−4)
1 12	5.25(−3)	3.56(−3)	2.54(−3)	1.36(−3)
1 13	7.32(−3)	4.95(−3)	3.52(−3)	1.86(−3)
1 14	1.78(−1)	1.71(−1)	1.64(−1)	1.48(−1)
1 15	1.35(−3)	8.93(−4)	6.18(−4)	3.02(−4)
1 16	1.05(−1)	1.10(−1)	1.12(−1)	1.14(−1)
2 3	9.41(−3)	6.55(−3)	4.80(−3)	2.70(−3)
2 4	9.00(−2)	8.51(−2)	8.06(−2)	7.13(−2)
2 5	1.47(−3)	9.89(−4)	7.06(−4)	3.79(−4)
2 6	4.03(−3)	2.74(−3)	1.97(−3)	1.08(−3)
2 7	8.08(−4)	5.45(−4)	3.93(−4)	2.17(−4)
2 8	1.46(0)	1.58(0)	1.68(0)	1.85(0)
2 9	4.34(−4)	3.28(−4)	2.60(−4)	1.69(−4)
2 10	1.39(−4)	9.21(−5)	6.53(−5)	3.53(−5)
2 11	1.03(0)	1.12(0)	1.20(0)	1.33(0)
2 12	3.07(−3)	2.05(−3)	1.45(−3)	7.69(−4)
2 13	1.36(−2)	1.33(−2)	1.31(−2)	1.23(−2)
2 14	1.48(−3)	9.80(−4)	6.88(−4)	3.57(−4)
2 15	9.50(−3)	1.25(−2)	1.56(−2)	2.30(−2)
2 16	2.05(−4)	1.23(−4)	8.01(−5)	3.62(−5)
3 4	2.11(−1)	1.97(−1)	1.85(−1)	1.61(−1)
3 5	6.98(−3)	5.37(−3)	4.36(−3)	3.09(−3)
3 6	4.29(−1)	4.62(−1)	4.92(−1)	5.45(−1)
3 7	1.55(0)	1.66(0)	1.75(0)	1.91(0)
3 8	1.12(0)	1.20(0)	1.27(0)	1.40(0)
3 9	1.35(0)	1.46(0)	1.57(0)	1.74(0)
3 10	9.41(−3)	9.91(−3)	1.04(−2)	1.31(−2)
3 11	7.98(−1)	8.63(−1)	9.15(−1)	1.01(0)
3 12	2.26(0)	2.46(0)	2.64(0)	2.97(0)
3 13	3.15(−2)	2.94(−2)	2.80(−2)	2.53(−2)
3 14	2.43(−2)	2.47(−2)	2.54(−2)	2.77(−2)
3 15	2.47(−2)	3.97(−2)	4.96(−2)	7.21(−2)
3 16	7.48(−4)	5.33(−4)	4.25(−4)	3.32(−4)

TABLE V. (*Continued*).

Transition $i \rightarrow j$		26.95 Ry	50.38 Ry	64.14 Ry	96.21 Ry
4	5	9.25(−3)	6.58(−3)	4.97(−3)	3.05(−3)
4	6	9.39(−1)	1.01(0)	1.06(0)	1.17(0)
4	7	9.38(−4)	6.80(−4)	5.23(−4)	3.24(−4)
4	8	1.98(0)	2.12(0)	2.23(0)	2.42(0)
4	9	4.61(0)	4.97(0)	5.27(0)	5.81(0)
4	10	1.66(−3)	1.11(−3)	7.95(−4)	4.35(−4)
4	11	8.27(−2)	8.61(−2)	8.89(−2)	9.36(−2)
4	12	8.36(−1)	9.01(−1)	9.56(−1)	1.06(0)
4	13	4.07(0)	4.48(0)	4.83(0)	5.48(0)
4	14	8.32(−3)	5.93(−3)	4.57(−3)	3.08(−3)
4	15	5.42(−2)	7.50(−2)	9.46(−2)	1.35(−1)
4	16	1.02(−3)	6.15(−4)	4.00(−4)	1.84(−4)
5	6	2.63(0)	2.85(0)	3.02(0)	3.32(0)
5	7	2.45(−2)	2.57(−2)	2.69(−2)	2.88(−2)
5	8	1.21(−2)	1.14(−2)	1.11(−2)	1.11(−2)
5	9	5.73(−1)	6.19(−1)	6.57(−1)	7.24(−1)
5	10	1.86(0)	1.99(0)	2.11(0)	2.31(0)
5	11	1.10(−2)	9.70(−3)	9.02(−3)	8.49(−3)
5	12	1.44(−2)	1.20(−2)	1.08(−2)	9.58(−2)
5	13	1.20(−2)	8.01(−3)	5.68(−3)	3.02(−3)
5	14	6.61(0)	7.24(0)	7.77(0)	8.74(0)
5	15	1.73(−3)	1.24(−3)	1.03(−3)	9.77(−4)
5	16	2.60(−2)	3.64(−2)	4.64(−2)	6.78(−2)
6	7	3.79(−2)	3.42(−2)	3.17(−2)	2.72(−2)
6	8	4.59(−2)	3.64(−2)	3.23(−2)	2.63(−2)
6	9	1.65(−1)	1.54(−1)	1.43(−1)	1.25(−1)
6	10	1.63(−1)	1.54(−1)	1.47(−1)	1.30(−1)
6	11	2.30(−3)	1.47(−3)	1.01(−3)	5.16(−4)
6	12	3.99(−3)	2.56(−3)	1.76(−3)	8.93(−4)
6	13	5.91(−3)	3.83(−3)	2.66(−3)	1.38(−3)
6	14	2.07(−2)	1.87(−2)	1.73(−2)	1.52(−2)
6	15	6.01(−4)	3.84(−4)	2.60(−4)	1.22(−4)
6	16	4.00(−3)	3.34(−3)	2.66(−3)	1.64(−3)
7	8	1.55(−2)	7.07(−3)	5.11(−3)	2.82(−3)
7	9	5.30(−2)	4.78(−2)	4.51(−2)	3.97(−2)
7	10	2.15(−4)	1.37(−4)	9.18(−5)	4.47(−5)
7	11	2.45(−4)	1.68(−4)	1.20(−4)	6.28(−5)
7	12	9.05(−4)	8.17(−4)	7.39(−4)	5.99(−4)
7	13	1.84(−5)	1.42(−5)	1.15(−5)	7.90(−6)
7	14	2.51(−3)	2.14(−3)	1.90(−3)	1.55(−3)
7	15	1.80(−5)	1.50(−5)	1.19(−5)	6.71(−6)
7	16	1.36(−5)	1.29(−5)	1.26(−5)	1.20(−5)
8	9	1.72(−1)	1.49(−1)	1.39(−1)	1.20(−1)
8	10	1.07(−3)	6.64(−4)	4.52(−4)	2.25(−4)
8	11	1.47(−3)	1.30(−3)	1.16(−3)	9.21(−4)
8	12	7.84(−4)	5.91(−4)	4.66(−4)	3.04(−4)
8	13	1.37(−3)	1.23(−3)	1.12(−3)	9.06(−4)
8	14	2.56(−3)	1.75(−3)	1.26(−3)	6.89(−4)
8	15	5.32(−5)	4.45(−5)	3.55(−5)	2.02(−5)
8	16	2.87(−6)	1.63(−6)	1.02(−6)	4.30(−7)
9	10	5.00(−3)	4.76(−2)	4.49(−2)	3.96(−2)
9	11	1.00(−3)	7.33(−4)	5.71(−4)	3.74(−4)
9	12	2.54(−3)	2.02(−3)	1.68(−3)	1.22(−3)
9	13	4.16(−3)	3.26(−3)	2.68(−3)	1.92(−3)
9	14	6.64(−3)	5.11(−3)	4.23(−3)	3.16(−3)
9	15	2.11(−4)	1.48(−4)	1.07(−4)	5.47(−5)
9	16	8.90(−4)	7.40(−4)	5.90(−4)	3.65(−4)
10	11	1.20(−4)	7.71(−5)	5.38(−5)	2.81(−5)
10	12	3.24(−4)	2.48(−4)	2.02(−4)	1.46(−4)

TABLE V. (*Continued*).

Transition $i \rightarrow j$		26.95 Ry	50.38 Ry	64.14 Ry	96.21 Ry
10	13	2.98(−4)	1.95(−4)	1.36(−4)	7.11(−5)
10	14	7.09(−2)	6.68(−2)	6.32(−2)	5.58(−2)
10	15	9.02(−6)	5.50(−6)	3.57(−6)	1.60(−6)
10	16	1.30(−4)	1.18(−4)	1.10(−4)	9.84(−5)
11	12	1.10(−1)	9.63(−2)	8.72(−2)	7.36(−2)
11	13	2.70(−2)	2.31(−2)	2.10(−2)	1.85(−2)
11	14	1.16(−2)	7.26(−3)	4.88(−3)	2.37(−3)
11	15	8.51(−3)	6.58(−3)	5.18(−3)	3.54(−3)
11	16	5.51(−4)	3.41(−4)	2.25(−4)	1.03(−4)
12	13	1.37(−1)	1.19(−1)	1.08(−1)	9.14(−2)
12	14	1.92(−2)	1.21(−2)	8.10(−3)	3.93(−3)
12	15	1.51(−2)	1.21(−2)	9.45(−3)	6.18(−3)
12	16	9.19(−4)	5.68(−4)	3.76(−4)	1.73(−4)
13	14	2.68(−2)	1.68(−2)	1.13(−2)	5.47(−3)
13	15	2.31(−2)	1.88(−2)	1.50(−2)	9.16(−3)
13	16	1.29(−3)	7.94(−4)	5.24(−4)	2.43(−4)
14	15	2.10(−3)	1.31(−3)	8.66(−4)	4.02(−4)
14	16	7.76(−3)	6.37(−3)	5.15(−3)	3.50(−3)
15	16	2.12(−3)	1.28(−3)	8.18(−4)	3.81(−4)

thors. The comparison is made at two energies that are rather close in the two sets of calculations; therefore the difference due to this fact should be relatively small. The present work confirms the large cross section for excitation of the $3p^2\,{}^3P_2$ state obtained by Bhatia and Kastner,[12] lending support to their argument that the term energy for this state should be corrected to 581 500 cm^{-1}. This state yields two relatively strong lines that, in their analysis of line emission, are quite sensitive to electron densities when it exceeds 10^8–10^9 cm^{-3}. We find, however, that for a majority of the transitions there are significant discrepancies, particularly at the higher energy. Most of the differences are greater than 25%, and are more than a factor of 2 for many of the transitions.

The discrepancies for the dipole- and spin-allowed transitions are particularly significant since the collision strengths given by Bhatia and Kastner, for most such transitions, *decrease* in value as the incident electron energy increases (Bhatia and Kastner have also calculated the collision strengths at 8.0 Ry and the same trend is seen). This is contrary to the expected behavior for dipole-allowed transitions where, due to the contribution from higher partial waves, the collision strengths should increase with energy (as in the present work). We also find large discrepancies for some nondipole transitions; for example, the transition $3s^2\,{}^1S_0$–$3p^2\,{}^3P_2$, where our value is nearly a factor of 2 higher at the higher energy in Table IV.

In their work Bhatia and Kastner adopted a rather restricted basis set of eigenfunctions to represent the target states, including only the configurations $3s^2$, $3s\,3p$, $3p^2$, and $3s\,3d$. On the other hand, as described in Sec. II, we use a large basis set involving 20 configurations and therefore our target states should be more accurately represented. One indication of the accuracy is that our dipole line strengths in Table II are in much better agreement with the relativistic calculations of Cheng and Johnson.[21] The configuration mixing affects the IC collision strengths in the following manner. Taking the transition $3s^2\,{}^1S_0$–$3p^2\,{}^3P_2$ as an example, Bhatia and Kastner give the composition of their ${}^3P_2$ state as

$$|\,3p^2\,{}^3P_2\rangle = (0.003)^2\,|\,3s\,3d\,{}^3D_2\rangle + (0.315)^2\,|\,3p^2\,{}^1D_2\rangle + (0.185)^2\,|\,3s\,3d\,{}^1D_2\rangle + (0.931)^2\,|\,3p^2\,{}^3P_2\rangle \tag{5}$$

(note that there is considerable mixing with the ${}^1D_2$ levels, which have a larger collision strength for excitation from the ground state, a point first made by Bhatia and Kastner[12]). With the configurations listed in Sec. II, our composition of the same state is

$$\begin{aligned}|\,3p^2\,{}^3P_2\rangle = {} & (0.0030)^2\,|\,3s\,3d\,{}^3D_2\rangle + (0.0001)^2\,|\,3s\,4d\,{}^3D_2\rangle + (0.0012)^2\,|\,3p\,4p\,{}^3D_2\rangle \\ & + (0.0001)^2\,|\,3p\,4f\,{}^3D_2\rangle + (0.3500)^2\,|\,3p^2\,{}^1D_2\rangle + (0.1986)^2\,|\,3s\,3d\,{}^1D_2\rangle \\ & + (0.0028)^2\,|\,3s\,4d\,{}^1D_2\rangle + (0.0063)^2\,|\,3p\,4p\,{}^1D_2\rangle + (0.0004)^2\,|\,3p\,4f\,{}^1D_2\rangle \\ & + (0.0129)^2\,|\,3d^2\,{}^1D_2\rangle + (0.0011)^2\,|\,4p^2\,{}^1D_2\rangle + (0.0001)^2\,|\,4d^2\,{}^1D_2\rangle \\ & + (0.9133)^2\,|\,3p^2\,{}^3P_2\rangle + (0.0184)^2\,|\,3p\,4p\,{}^3P_2\rangle + (0.0580)^2\,|\,3d^2\,{}^3P_2\rangle \\ & + (0.0006)^2\,|\,3d\,4d\,{}^3P_2\rangle + (0.0030)^2\,|\,4p^2\,{}^3P_2\rangle + (0.0005)^2\,|\,4d^2\,{}^3P_2\rangle\ . \end{aligned} \tag{6}$$

From the above expansion, one can readily see the configurations that mix significantly (Bhatia and Kastner do not, for example, include the $3d^2$ configuration that makes an appreciable contribution to the total wave function). The mixing with the $^1D_2$ states is seen to be larger in our case, partially accounting for our higher collision strengths for the $3s^2\,^1S_0-3p^2\,^3P_2$ transition.

Our results for transitions from the ground state are compared with those of Mann[13] in Fig. 1. In this case we sum over J of the final state, as Mann does not publish results for individual fine-structure transitions (these are, however, available[13]). The agreement is remarkably good, considering that different approaches to the DW approximation were used in the two calculations. The sole exception is the collision strength for excitation of the $3s\,3d\,^1D$ state, where our result is $\sim 60\%$ of Mann's at the highest energy. This is partially due (about 20% of the difference[13]) to mixing of the $3d^2$ configuration in the final state, which we find to have a (squared) coefficient of 0.010, but which was originally not included by Mann. Other configurations unique to the present final state ($3s\,4d, 3p\,4f$) may account for the remainder.

There have also been other calculations for Fe XV in LS coupling[10,11] without the consideration of autoionizing resonances. We do not make a detailed comparison with these calculations since, as we have seen, the IC effect has a considerable role in the cross sections for a majority of the transitions. However, an overall survey of the earlier LS calculations does show that for dipole transitions weakly affected by IC (e.g., $3s^2\,^1S_0-3s\,3p\,^1P_1$), the agreement with the present results is better than 20%.

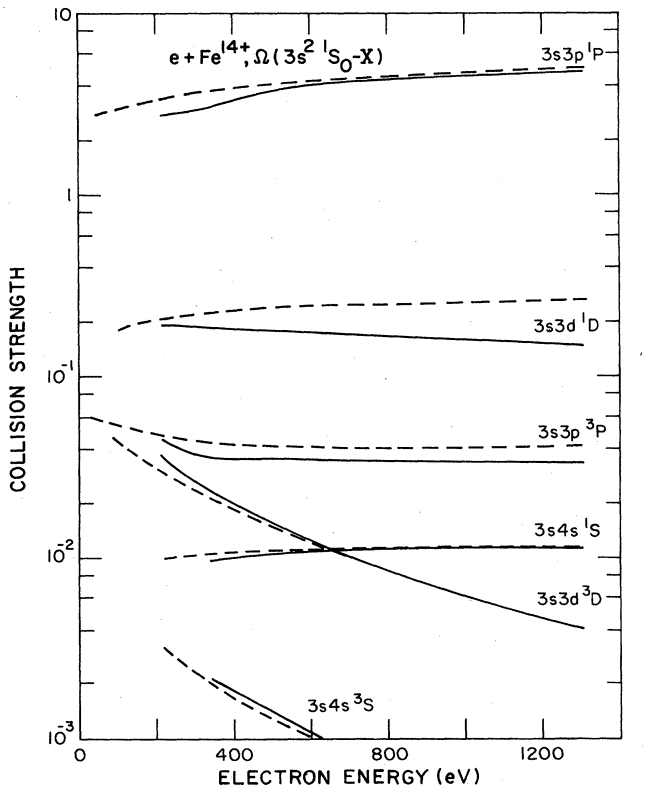

FIG. 1. Collision strengths for transitions from the ground state ($3s^2\,^1S_0$) summed over all final-state J values: present work (——); Ref. 13 (— — —).

As mentioned in Sec. I, it has been shown that for the lower members of the Mg sequence autoionization plays an important role in the enhancement of the effective collision strengths for some transitions. In addition to the nonresonant results given in Tables IV and V, we also consider the resonance structures lying in the energy regions bounded by the various thresholds. We divide the resonance calculations according to the different energy ranges determined by a given number of open channels in each range. All fine-structure levels are considered degenerate and, in addition, the LS terms $3p^2\,^1D$ and ^3P are treated as degenerate (the energies are close together), as well as the terms $3p^2\,^1S$ and $3s\,3d\,^3D$. As described in Sec. II, the $\mathbf{R}$ matrices calculated in LS coupling above each threshold(s) are extrapolated to energies below threshold(s). The transformation to IC is then carried out and the detailed collision strengths with resonance structures are obtained using QDT formulas.

We consider in detail here only the transition $3s^2\,^1S_0-3s\,3p\,^3P_1$. A glance at the tables of collision strengths from the ground state reveals that by far the largest collision strength is to the level $3s\,3p\,^1P_1$. Therefore, we expect the largest autoionization contribution from the Rydberg series of resonances lying in the energy region $3s\,3p\,^3P_1-3s\,3p\,^1P_1$, converging onto the latter state. $\mathbf{R}^{LS}$ are accordingly calculated at a few points above the $3s\,3p\,^1P_1$ threshold ($k_1^2=3.10$, 3.15, 3.25 Ry) and extrapolated to energies below threshold ($k_1^2=2.2$, 2.6, 3.0 Ry).

One may define the effective quantum number as an energy variable as follows:

$$\nu = z[E(3s\,3p\,^1P_1)-E]^{-1/2}\,, \tag{7}$$

and calculate the collision strengths as a function of ν, rather than E. The reason for this choice is that in a collision strength with complicated resonance structures $\Omega(\nu)$ is more spread out (and hence exhibits more detail) than $\Omega(E)$. Furthermore, as we shall see, the resonance structure repeats itself, with nearly identical form, for each interval $\Delta\nu=1$ (some variation is expected due to the slow energy dependence of the extrapolated $\mathbf{R}^{LS}$ matrices).

From (7) we find that the effective quantum number of the $3s\,3p\,^3P_1$ level relative to the $3s\,3p\,^1P_1$ level is 14.11. $\mathbf{R}^{LS}$ matrices at $k_1^2=2.2$ ($\nu=15.07$) are employed to obtain the detailed collision strengths in the range $14.11\le\nu<16.11$ ($k_1^2=2.31$ Ry). In Fig. 2 we plot $\Omega(3s^2\,^1S_0-3s\,3p\,^3P_1)$ in this energy range. The two resonance groups shown in Fig. 2 have, as pointed out earlier, nearly identical form as a function of ν. As a function of E, however, one would expect the resonance structure, corresponding to each $\Delta\nu=1$ range, to cover a smaller and smaller ΔE range (with increasing ν), and get contracted due to decreasing resonance widths. The collision strengths plotted in Fig. 2 includes the contribution from all $LS\pi$ symmetries that add up to total $J\pi$ states with $J\le\frac{11}{2}$. Resonance contributions from higher angular symmetries are negligible; however, the background con-

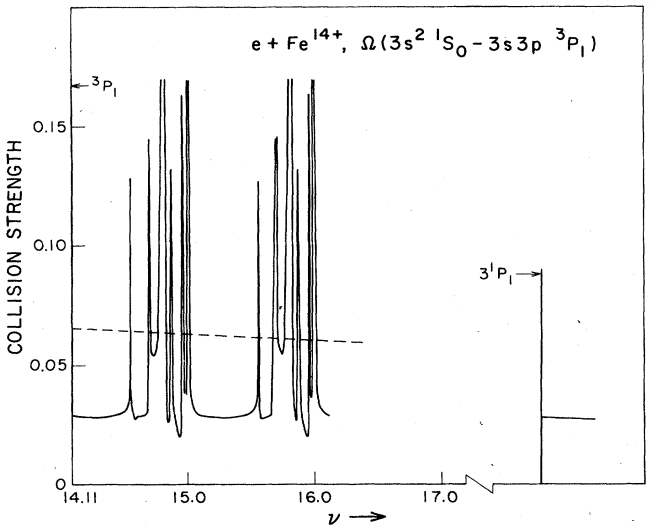

FIG. 2. The collision strength for the transition $3s^2\,{}^1S_0$—$3s\,3p\,{}^3P_1$ showing the autoionization structure corresponding to the two lowest groups of resonances converging onto the $3\,{}^1P_1$ threshold. The dashed line is the Gailitis average over the resonances. The abscissa is the effective quantum number defined by Eq. (7).

tribution from the higher partial waves ($J > \frac{11}{2}$) is approximately 17% of that shown in Fig. 2. The dashed line indicates the Gailitis average over the resonance structures. A number of other transitions, mainly forbidden ones, also show considerable resonance structure and resulting enhancement in the collision strength.

The effect of term coupling on the $3s^2\,{}^1S_0$—$3s\,3p\,{}^3P_1$ transition is even more pronounced than the effect of resonances. For instance, at the energies $k_1^2 = 15.918$ Ry and $k_1^2 = 96.21$ Ry, we have $\Omega(LS) = 0.0078$ and 0.001, respectively, whereas $\Omega(\mathrm{IC}) = 0.0203$ and 0.0061, respectively (the values given are for partial wave summation involving $l \leq 10$, since for higher partial waves we use a Coulomb-Bethe scheme). At a lower energy, $k_1^2 = 3.10$, $\Omega(LS) = 0.015$, and $\Omega(\mathrm{IC}) = 0.023$, i.e., a much smaller IC effect. This trend is typical of the behavior of a collision strength for an intercombination-type transition where, for high Z, the triplet level mixes with the singlet level (the transition to the singlet being an allowed one). The transition does not begin to be dominated by the mixing of the singlet and triplet levels until the collision energy exceeds 100 Ry, whereafter the collision strength displays[13] the increasing behavior typical of a dipole-allowed transition. In Ref. 16 we have discussed, in some detail, the energy behavior of the 1^1S_0-2^3P_1 intercombination transition in high-Z He-like ions.

The values for the effective collision strength of the $3s^2\,{}^1S_0$—$3s\,3p\,{}^3P_1$ transition in the threshold region are critical to the calculated intensity ratio of this line with that from resonance excitation ($3s^2\,{}^1S_0$—$3s\,3p\,{}^1P_1$). The present result is approximately 0.064; the results of earlier calculations are smaller: 0.056 (Ref. 7), 0.027 (Ref. 9), approximately 0.024 (Ref. 12), and 0.033 (Ref. 13). As noted above, only the present work and that of Bely and Blaha[7] included any contribution from resonances.

The ratio of the intensities of the intercombination line, at 417.3 Å, to the resonance line, at 284.2 Å, has been observed[29] to be approximately 0.027 in the Sun, but calculated to be 0.035 and 0.040 in Refs. 7 and 12, respectively. A significant difference showed up, however, when the results of Ref. 12 for $_{26}$Fe XV and $_{28}$Ni XVII were extrapolated and compared with observations of the ratio in three other Mg-like ions;[3] the measured intensity ratios were more than three times larger than predicted.[30] In computing this line ratio, Bely and Blaha did not allow for cascade from the $3s\,3d\,{}^3D_{1,2}$ or $3p^2\,{}^3P_2$ levels as a populating mechanism for the $3s\,3p\,{}^3P_1$ state, as suggested later.[9,12] Bhatia and Kastner[12] included these effects, but with a much lower value for the $3s^2\,{}^1S_0$—$3s\,3p\,{}^3P_1$ cross section; their result for this line ratio was thus in agreement with that of Bely and Blaha.

Use of the present results in a complete reanalysis of the Fe XV emission would undoubtedly lead to a significant increase in the 417.3/284.2 line ratio. Our collision strength for the $3s^2\,{}^1S_0$—$3s\,3p\,{}^3P_1$ transition is about three times larger at threshold than that of Bhatia and Kastner, and those for exciting the important cascade states are also significantly larger. This would aggravate the disagreement between the calculated values and those measured in the Sun, but tend to reduce the discrepancy for the laboratory data. Independent of any calculation, it appears that the solar and laboratory measurement are inconsistent.

IV. CONCLUDING REMARKS

We have calculated the collision strengths in intermediate coupling for a number of transitions in Fe XV at energies up to several times the threshold energies. In the nonresonant energy region we find significant differences with the work of Bhatia and Kastner[12,28] for both the allowed and the nonallowed transitions, but generally good agreement with the work of Mann[13] for transitions from the ground state. Resonance effects have been considered, using quantum-defect theory, in the energy regions lying between the various states included in the target representation. Calculation of the collisional rate coefficients is in progress, including further work on the detailed analysis of resonances for all transitions affected thereby. For the optically allowed transitions, the resonance effects are small (with the exception of the $3s^2\,{}^1S_0$—$3s\,3p\,{}^3P_1$ transition) and the present collision strengths could be readily employed immediately to obtain the corresponding rate coefficients.

Future work will also include detailed calculations of line intensities for use in plasma modeling. There are a large number of transitions that display considerable sensitivity to electron density;[12,31] absolute intensities may also provide a useful diagnostic tool when the strong resonance line is either blended or beyond the range of measuring apparatus.[3,4] We also have in progress similar calculations for several other highly ionized Mg-like ions, so that data for other species will ultimately be available.

Note added in proof. It has been brought to our attention [J. B. Mann (private communication)] that the collision strength for the transition $3s^2\,{}^1S-3s\,3d\,{}^1D$ does not converge for $l \leq 11$ for all energies considered in the present work except the lowest one (15.918 Ry). The additional contribution from $l > 11$ (up to about $l \approx 80$ according to Mann's calculations), rather than additional configuration interaction, is the reason for the $\sim 75\%$ discrepancy for this transition in Fig. 1. The corrections, estimated from Mann's results, to the values given in Tables IV and V are by factors of 1.07, 1.17, 1.30, 1.41, 1.51, and 1.70 for the six energies, respectively. Other transitions with associated quadrupole moments may also involve some additional contributions from higher partial waves (although to a smaller extent since the strength of other such transitions is much weaker).

ACKNOWLEDGMENTS

This work was supported by the U. S. Department of Energy (Office of Fusion Energy). We are pleased to acknowledge very helpful communications from J. B. Mann, A. K. Bhatia, E. Hinnov, H. W. Moos, M. Finkenthal, and W. R. Johnson.

---

*Present address: Lawrence Livermore National Laboratory, L-35, University of California, Livermore, CA 94550.

†Quantum Physics Division, National Bureau of Standards, Boulder, CO 80309.

[1]G. A. Doschek, U. Feldman, M. E. Hoosier, and J. D. F. Bartoe, Astrophys. J. Suppl. Ser. **31**, 417 (1976).

[2]J. E. Vernazza and E. M. Reeves, Astrophys. J. Suppl. Ser. **37**, 485 (1978).

[3]M. Finkenthal, R. E. Bell, H. W. Moos, and TFR Group, Phys. Lett. **88A**, 165 (1982).

[4]M. Finkenthal, E. Hinnov, S. Cohen, and S. Suckewer, Phys. Lett. **91**, 284 (1982).

[5]K. L. Baluja, P. G. Burke, and A. E. Kingston, J. Phys. B **13**, L543 (1980); **14**, 1333 (1981).

[6]P. L. Dufton and A. E. Kingston, J. Phys. B **17**, 3321 (1984).

[7]O. Bely and M. Blaha, Sol. Phys. **3**, 563 (1968).

[8]D. R. Flower, J. Phys. B **4**, 697 (1971).

[9]D. R. Flower and C. Jordan, Astron. Astrophys. **14**, 473 (1971).

[10]J. Davis, P. C. Kepple, and M. Blaha, J. Quant. Spectrosc. Radiat. Transfer **16**, 1043 (1976).

[11]S. M. Younger, J. Quant. Spectrosc. Radiat. Transfer **23**, 489 (1980).

[12]A. K. Bhatia and S. O. Kastner, Sol. Phys. **65**, 181 (1980).

[13]J. B. Mann, At. Data Nucl. Data Tables **29**, 407 (1983); and private communication.

[14]W. Eissner, in *Proceedings of the Seventh International Conference on the Physics of Electronic and Atomic Collisions, Amsterdam, 1971,* edited by T. Govers and F. J. De Heer (North-Holland, Amsterdam, 1972), p. 460.

[15]A. K. Pradhan, D. W. Norcross, and D. G. Hummer, Phys. Rev. A **23**, 619 (1981).

[16]A. K. Pradhan, Phys. Rev. A **28**, 2113 (1983).

[17]A. K. Pradhan, Phys. Rev. A **28**, 2128 (1983).

[18]A. K. Pradhan, Phys. Rev. A **30**, 100 (1984).

[19]W. Eissner, M. Jones, and H. Nussbaumer, Comput. Phys. Commun. **8**, 270 (1974).

[20]C. Corliss and J. Sugar, J. Phys. Chem. Ref. Data **11**, 213 (1982).

[21]K. T. Cheng and W. R. Johnson, Phys. Rev. A **16**, 263 (1977).

[22]J. R. Fuhr, G. A. Martin, W. L. Wiese, and S. M. Younger, J. Phys. Chem. Ref. Data **10**, 305 (1981).

[23]M. Smith and W. L. Wiese, J. Phys. Chem. Ref. Data **2**, 85 (1973).

[24]H. E. Saraph, Comput. Phys. Commun. **15**, 247 (1978); **3**, 256 (1972).

[25]A. Burgess and V. B. Sheorey, J. Phys. B **7**, 2403 (1974).

[26]P. de A. P. Martins and M. J. Seaton, J. Phys. B **2**, 333 (1969).

[27]M. Gailitis, Zh. Eksp. Teor. Fiz. **44**, 1974 (1963) [Sov. Phys.—JETP **17**, 1328 (1963)].

[28]A. K. Bhatia and S. O. Kastner, J. Quant. Spectrosc. Radiat. Transfer **24**, 53 (1980).

[29]L. A. Hall and H. E. Hinteregger, J. Geophys. Res. **75**, 6959 (1970); the ratio 0.062 reported by these authors is modified here in recognition of the demonstration [J. D. Purcell and K. G. Widing, Astrophys. J. **176**, 239 (1972)] that the 417.3-Å line of $_{26}$Fe XV is actually blended with a line of $_{14}$Si XIV of "comparable intensity."

[30]The authors of Ref. 3 incorrectly compared the ratio of measured flux with calculated ratios of intensities, which differ by a factor of the ratio of the photon energies. The logs of the correct intensity ratios for the three ions considered in Ref. 3 are all approximately -1.2, reducing the discrepancy to a still substantial factor of 2–3.

[31]K. P. Dere, D. M. Horan and R. W. Kreplin, Astrophys. J. **217**, 976 (1977).